Density Functional Calculations, Synthesis, and Characterization on Two Novel Quadruple Hydrogen-Bonded Supramolecular Complexes

Fang F. Jian,*,†,‡ Pu S. Zhao,†,‡ Qing Yu,† Qing X. Wang,† and Kui Jiao†

New Materials and Function Coordination Chemistry Laboratory, Qingdao University of Science and Technology, Qingdao Shandong 266042, People's Republic of China, and Materials Chemistry Laboratory, Nanjing University of Science and Technology, Nanjing 210094, People's Republic of China

Received: December 18, 2003; In Final Form: April 19, 2004

Two novel quadruple hydrogen-bonded supramolecular structure 1:2 adducts of dimethylglyoxime·benzoic acid and dimethylglyoxime·cinnamic acid have been designed and optimized at the B3LYP/6-31G* level. The calculated results show that, at a temperature of 298.15 K and pressure of 0.1 MPa, the changes in the Gibbs free energy (ΔG_T) for the two aggregations from monomers to corresponding trimers are −41.7 and −42.7 kJ/mol, respectively, which imply that the processes of forming the trimers are spontaneous. Based on this design, we have synthesized the anticipatory supramolecular compounds successfully by selecting catalysts, and their crystal structures closely resemble the optimized structures. The predicted vibrational frequencies are in good agreement with the experimental values. Thermal stability analyses demonstrate that these two supramolecular compounds are new complexes and they are not the ordinary superposition of the original monomers.

1. Introduction

Supramolecular chemistry may be defined as "chemistry beyond the molecular", bearing on the organized entities of higher complexity that result from the association of two or more chemical species held together by intermolecular noncovalent forces, including hydrogen bonding, electrostatic interaction, van der Waals forces, short-range exclusion forces, etc.[1] Supramolecular compounds with special structures and functions have wide application in various fields such as material, catalysis, conductor, semiconductor, medicine, and biotechnology.[2−4] The highly selective and directional nature and appropriate strength of the hydrogen bond make it ideal for use in the construction and stabilization of large noncovalently linked molecular and supramolecular architectures.[5] Recently, the assembly of supramolecular compounds that have special structure and function from simple building blocks, directed by hydrogen-bond formation, has attracted widespread attention, and several research groups have attempted to control molecular architectures using hydrogen-bond networks.[6−8] To construct a supramolecular aggregate successfully, it is important to choose the building blocks that have appropriate hydrogen binding sites. Some organic molecules, such as 2-acrylamidopyridine,[9] 2,6-diamidopyridne, 2-aminopyrimidine, barbituric acid, 2,4,6-triaminopyrimidine carboxylic acids, and dicarboxylic acids and their derivatives[5] are ideal building blocks, because they have appropriate hydrogen-bond donors and acceptors. They have been used to construct molecular aggregations that have led to the design and synthesis of many particular supramolecular materials in which the components are held together by arrays of double, triple, quadruple, or quintuple hydrogen bonds.[10−12]

However, until now, we have not found a report about the dimethylglyoxime (DIMG) that acts as a building block. In fact, DIMG is a potential hydrogen-bond building block, because the hydroxyl group can act as hydrogen-bond donor site and the N atom can act as a hydrogen-bond acceptor site. To verify this thought, we designed some heterotrimer supramolecules that were connected by quadruple hydrogen bonds consisting of one DIMG as the donor−acceptor−acceptor−donor (DAAD) unit and two carboxylic acids as acceptor−donor (AD) units (see Figures 1 and 2) and we applied the density functional theory (DFT) method B3LYP/6-31G* to optimize the geometry of the proposed structures. It is well-known, with the vast development of computational chemistry in the past decade, that the theoretical modeling of supramolecular chemistry has become much more mature than ever. Many important chemical and physical properties of the chemical system can be predicted from first principles by various computational techniques.[13] DFT has long been recognized as a better alternative tool in the study of organic chemical systems than the ab initio methods used in the past,[14] because of the fact it is computationally less demanding for inclusion of electron correlation. Detailed analyses[15−21] on the performance of different DFT methods had been performed, particularly for equilibrium structure properties of molecular systems, such as geometry, dipole moment, vibrational frequency, etc. The general conclusion from these studies was that DFT methods, particularly with the use of nonlocal exchange-correlation functions, can predict accurate equilibrium structure properties. DFT has been used to study the structures and stability of hydrogen-bond complexes.[22] Zhang and co-workers have also used DFT calculations in multiple hydrogen-bond systems.[23]

With the aforementioned studies, we have chosen to conduct DFT calculations on the supramolecular complexes that we proposed, and the calculated results provide theoretical references for our original design idea. Subsequently, we have synthesized the anticipatory compounds successfully by controlling reaction conditions and selecting catalysts, and we have also obtained two crystal structures. Here, in this paper, we

* Author to whom correspondence should be addressed. Telephone: 0086-0532-4023606. Fax: 0086-0532-4023606. E-mail address: ffj2003@163169.net.

† Qingdao University of Science and Technology.

‡ Nanjing University of Science and Technology.

10.1021/jp037926o CCC: $27.50
Published on Web 05/22/2004

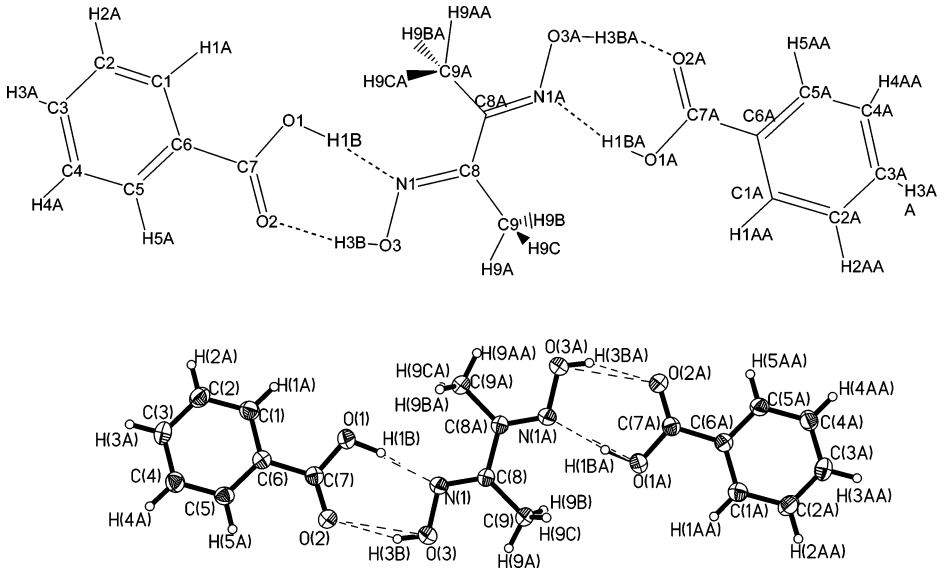

Figure 1. Proposed and experimental molecular structures of **1**, with the atomic numbering scheme shown.

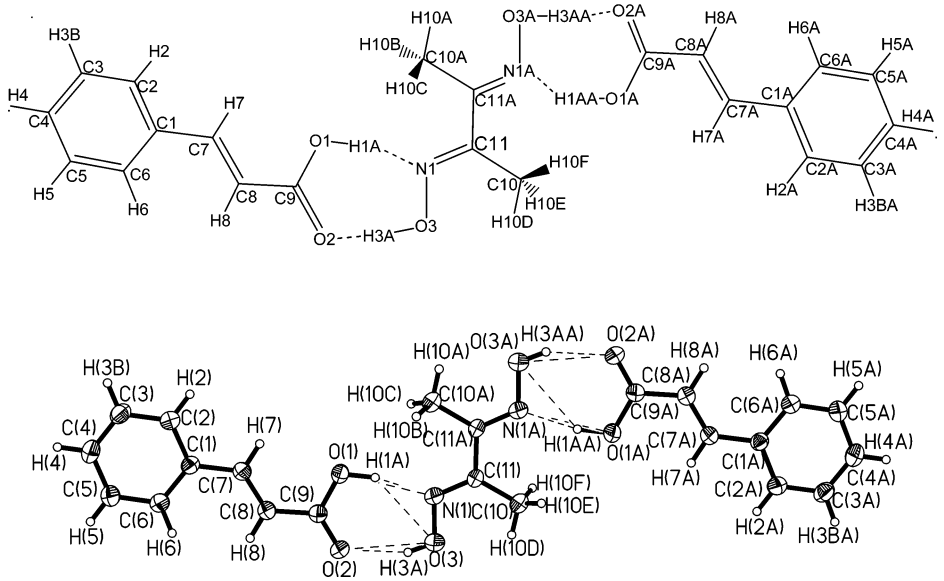

Figure 2. Proposed and experimental molecular structures of **2**, with the atomic numbering scheme shown.

report the DFT calculational results and the crystal structures of the two adducts as well as their IR spectra and thermal stability. Further investigations about the trimers that contain DIMG are in progress.

2. Computational and Experimental Methods

2.1. Computational Methods. All calculations were performed with Gaussian 98 software package[24] on a Pentium IV computer and a Compaq Alpha DS20E server, using the default convergence criteria.

Density functional calculations were all self-consistent Kohn−Sham calculations that used the B3LYP density functional. B3LYP combines the exchange functional of Becke's three parameters[25] with the correlation functional proposed by Lee, Yang, and Parr.[26] This functional has been shown to give geometries and energies comparable to second-order Møller−Plesset (MP2) levels of theory for a wide range of molecules.[20] It has also been shown to predict vibrational frequencies of comparable accuracy to experimental data.[27−29]

In terms of disk space, computer time, and the size of the molecules studied here, the standard 6-31G* Gaussian basis set due to Binkley, Pople, and co-workers[30,31] was used for B3LYP density functional calculation. Geometry optimizations were performed using the Berny gradient optimization method.[32] Normal-mode vibrational frequencies were calculated from the analytical harmonic force constants. Vibrational frequencies that were calculated to ascertain the structure was characterized to be the stable structure (no imaginary frequencies). Zero-point energy (ZPE) corrections were made to the interaction energies, and basis set superposition errors (BSSEs) were taken into consideration, using the Boys−Bernardi counterpoise procedure (CP).[33−36] Natural bond orbital (NBO) analyses[37] were performed on the optimized structure. Thermodynamic properties and their changes in the aggregation were derived from statistical thermodynamics based on the frequencies.

2.2. Synthesis. Compound **1** was prepared using the following procedure. $FeCl_3 \cdot 6H_2O$ (0.05 g, 0.2 mmol) and benzoic acid (BZA) (0.25 g, 2.0 mmol) were added to a warm solution of DIMG (0.12 g, 1.0 mmol) in ethyl alcohol (EtOH) (50.0 mL), with stirring, and the mixture was refluxed for 2 h. The brown−yellow solution then was filtered, and the filtrate was allowed to stand undisturbed. Upon slow evaporation at room temper-

TABLE 1: Summary of Crystallographic Results for the Compounds

property	Value	
	compound **1**	compound **2**
empirical formula	$C_{18}H_{20}N_2O_6$	$C_{22}H_{24}N_2O_6$
formula weight	360.36	412.44
temperature (K)	293(2)	293(2)
wavelength (Å)	0.71073	0.71073
crystal system, space group	$P2_1/c$, monoclinic	$P2_1/c$, monoclinic
unit cell dimensions		
a (Å)	8.8436(18)	5.5475(11)
b (Å)	5.3476(11	8.5902(17)
c (Å)	18.839(4)	22.232(5)
β (deg)	99.62(3)	98.52(3)
volume (Å^3)	878.4(3)	1047.7(4)
Z	2	2
calculated density (Mg/m^3)	1.362	1.307
absorption coefficient (mm^{-1})	0.103	0.096
F(000)	380	436
crystal size	0.4 mm × 0.4 mm × 0.7 mm	0.4 mm × 0.5 mm × 0.7 mm
θ range (deg)	2.19−27.52	1.85−27.51
limiting indices		
h	$0 \le h \le 11$	$0 \le h \le 6$
k	$-6 \le k \le 6$	$-10 \le k \le 10$
l	$-23 \le l \le 22$	$-28 \le l \le 27$
reflections collected/unique	2696/1665 ($R_{int} = 0.0438$)	1985/1227 ($R_{int} = 0.0396$)
completeness to $\theta = 27.52°$ (%)	82.5	50.9
refinement method	full-matrix least-squares on F^2	full-matrix least-squares on F^2
data/restraints/parameters	1665/0/123	1227/0/141
goodness-of-fit on F^2	1.059	1.128
final R indices [$I > 2\sigma(I)$]		
R_1	0.0511	0.0490
wR_2	0.1456	0.1024
R indices (all data)		
R_1	0.0801	0.0885
wR_2	0.1584	0.1102
extinction coefficient	0.031(7)	0.014(3)
largest diffraction peak and hole (e/Å^3)	0.240 and −0.227	0.132 and −0.142

TABLE 2: Atomic Coordinates and Equivalent Isotropic Displacement Parameter (U_{eq})[a] for Compound 1

atom	Atomic Coordinate (× 10^4)			U_{eq} (× 10^3 Å^2)	atom	Atomic Coordinate (× 10^4)			U_{eq} (× 10^3 Å^2)
	x	y	z			x	y	z	
O(1)	6376(2)	10692(3)	−1070(1)	53(1)	O(2)	8526(2)	11635(3)	−314(1)	55(1)
O(3)	7810(2)	7723(3)	501(1)	58(1)	N(1)	6459(2)	7173(3)	28(1)	42(1)
C(1)	7016(3)	14079(4)	−2089(1)	50(1)	C(2)	7321(3)	15910(5)	−2576(1)	56(1)
C(3)	8489(3)	17604(4)	−2371(2)	54(1)	C(4)	9358(3)	17485(5)	−1690(1)	50(1)
C(5)	9077(3)	15677(4)	−1207(1)	45(1)	C(6)	7900(3)	13957(4)	−1406(1)	40(1)
C(7)	7650(3)	12016(4)	−876(1)	42(1)	C(9)	6245(3)	3875(5)	924(1)	51(1)
C(8)	5721(2)	5311(4)	242(1)	37(1)					

[a] U_{eq} is defined as one-third of the trace of the orthogonalized U_{ij} tensor.

ature, a colorless crystalline solid appeared a week later and was separated by filtration. Yield: 85%, m.p. 152−154 °C. The carbon, hydrogen, and nitrogen content were determined by elemental analysis. (Calcd. for $C_{18}H_{20}N_2O_6$: C, 60.02; H, 5.55; N, 7.77. Found: C, 59.96; H, 5.61: N, 7.47.)

Compound **2** was prepared with the same procedure as that described for compound **1**, except that cinnamic acid (CINA) (0.30 g, 2.0 mmol) was used to replace the BZA. Yield: 82%, m.p. 170−172 °C. The carbon, hydrogen, and nitrogen content were determined by elemental analysis. (Calcd. for $C_{18}H_{20}N_2O_6$: C, 60.02; H, 5.55; N, 7.77. Found: C, 59.96; H, 5.61: N, 7.47.) $FeCl_3$ was used as a catalyst. We cannot obtain compound **1** or **2** if we mix DIMG directly with BZA or CINA in EtOH. We also used $ZnCl_2$, $CuSO_4$, $CoSO_4$, $CrCl_3$, and $CoCl_3$ as catalysts but did not obtain the expected product. The solids that we obtained were not the pure compounds; they were mixed compounds, without a fixed melting point. Also, the IR spectra were very different from those of the supramolecular complexes DIMG·2BZA or DIMG·2CINA. When we used $FeCl_2 \cdot 6H_2O$ as a catalyst, the melting points of the products were similar to those of the supramolecular complexes DIMG·2BZA and DIMG·2CINA and the IR spectra of the products also have similar peaks with those of the supramolecular complexes DIMG·2BZA and DIMG·2CINA. However, using only the IR spectra and melting points, we are not sure whether the products are supramolecular complexes or not. We shall do our best to obtain the single crystal.

2.3. X-ray Structure Determination. A summary of the key crystallographic information is given in Table 1. Atomic parameters and equivalent isotropic thermal parameters of non-H atoms for compounds **1** and **2** are given in Tables 2 and 3, respectively. The selected crystal of **1** and **2** was mounted on a Rigaku model Raxis-IV diffractometer. Reflection data were measured at 20 °C using graphite monochromated Mo Kα (λ = 0.71073 Å) radiation. The collected data were reduced using the program SAINT.[38] The structures were solved by direct methods and refined by a full-matrix least-squares method on F^2_{obs} using the SHELXTL software package.[39] All non-H

TABLE 3: Atomic Coordinates and Equivalent Isotropic Displacement Parameter (U_{eq})[a] for Compound 2

	Atomic Coordinate ($\times 10^4$)					Atomic Coordinate ($\times 10^4$)			
atom	*x*	*y*	*z*	U_{eq} ($\times 10^3$ Å^2)	atom	*x*	*y*	*z*	U_{eq} ($\times 10^3$ Å^2)
O(1)	−4545(4)	2392(3)	708(1)	68(1)	O(2)	−3343(4)	1535(3)	−134(1)	65(1)
O(3)	7238(4)	6873(3)	724(1)	68(1)	N(1)	7791(4)	6228(3)	190(1)	51(1)
C(1)	1047(5)	−35(4)	1830(1)	46(1)	C(2)	1069(5)	91(4)	2450(2)	56(1)
C(3)	2859(6)	−626(4)	2859(2)	62(1)	C(4)	4649(6)	−1483(4)	2657(2)	64(1)
C(5)	4662(6)	−1608(4)	2045(2)	65(1)	C(6)	2883(5)	−897(4)	1632(2)	60(1)
C(7)	−850(5)	742(4)	1408(2)	49(1)	C(8)	−1142(5)	753(4)	809(2)	53(1)
C(9)	−3071(5)	1575(4)	419(2)	49(1)	C(10)	11220(5)	5080(5)	883(1)	61(1)
C(11)	9690(5)	5363(4)	279(1)	42(1)					

[a] U_{eq} is defined as one-third of the trace of the orthogonalized U_{ij} tensor.

TABLE 4: Energies of the Monomers and Their Trimers with Different Basis Sets

	total energy, *E* (kJ/mol)	zero point energy, ZPE (kJ/mol)	basis set superposition error, BSSE (kJ/mol)	Interaction Energy (kJ/mol)[a]	
				uncorrected, ΔE	corrected, $\Delta E_{C,ZPEc}$
DIMG	−1093991.9 (−1094041. 4)	335.5 (334.8)			
BZA	−1103812.2 (−1103847.0)	304.4 (304.3)			
CINA	−1306834.0 (−1306877.1)	392.1 (391.7)			
compound **1**	−3301760.3 (−3301881.1)	955.0 (952.9)	32.5 (31.2)	−144.0 (−145.6)	−101.2 (−105.2)
compound **2**	- 3707805.2 (- 3707943.5)	1131.0 (1128.6)	32.9 (31.6)	−145.3 (−147.9)	−101.6 (−106.3)

[a] ΔE is the uncorrected interaction energy, and $\Delta E_{C,ZPEc}$ is the interaction energy corrected for BSSE and ZPE.

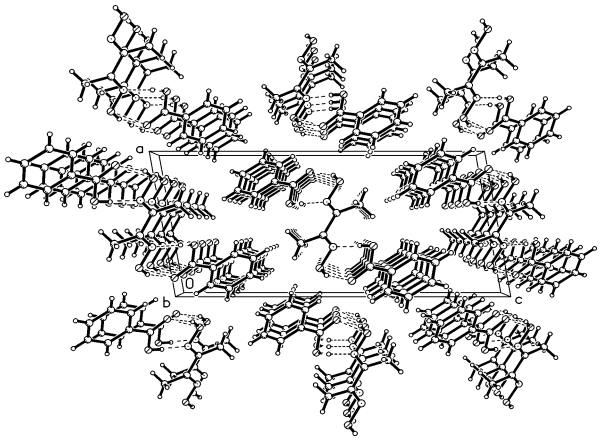

Figure 3. View of the crystal packing down the *b*-axis for **1**.

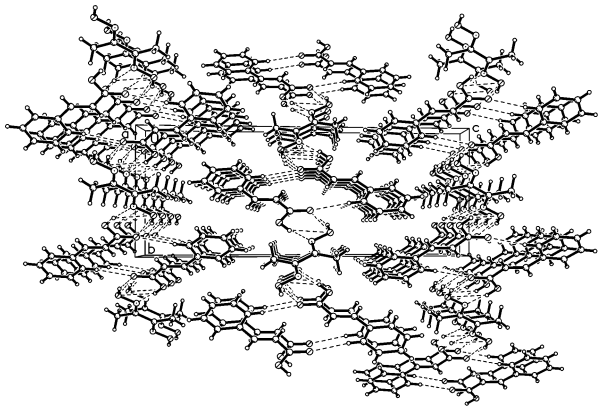

Figure 4. View of the crystal packing down the *a*-axis for **2**.

atoms were anisotropically refined. The positions of the H atom were fixed geometrically at calculated distances and allowed to ride on the parent C atoms. For **1**, the final least-squares cycle gave $R = 0.0511$, $R_w = 0.1456$ for 1209 reflections with $I > 2\sigma(I)$; the weighting scheme, $w = 1/[\sigma^2(F_o^2) + (0.0906P)^2]$, where $P = (F_o^2) + 2F_c^2)/3$. For **2**, the final least-squares cycle gave $R = 0.0490$, $R_w = 0.1024$ for 969 reflections with $I > 2\sigma(I)$; the weighting scheme was $w = 1/[\sigma^2(F_o^2) + (0.0426P)^2]$, where $P = (F_o^2 + 2F_c^2)/3$. Atomic scattering factors and anomalous dispersion corrections were taken from International Table for X-ray Crystallography data.[40]

3. Results and Discussion

3.1. Total Energies and Interaction Energies. The total energies and interaction energies calculated at the B3LYP/6-31G* and B3LYP/6-31G** levels for compounds **1** and **2** are given in Table 4, along with zero-point energies (ZPEs) and BSSE values. The values given in parentheses in the table are the calculated results with the 6-31G** basis set. The scaling factor for the calculated harmonic vibrational frequencies is 0.96.[41]

It can be seen that, at the B3LYP/6-31G* level, for compounds **1** and **2**, without BSSE and ZPE corrections, the total energy is much lower than the sum of energies of three monomers, by 144.0 and 145.3 kJ/mol, respectively. Even after correction, the energies of the compounds are still very low, which suggests that the compounds formed by BZA or CINA with DIMG can be subsistent and they are very stable. In addition, because the compounds are connected only by quadruple hydrogen bonds, all the interaction energies can be attributed (approximately) to these hydrogen bonds. The average energy per hydrogen bond then can be deduced, which is ∼25.3 kJ/mol for compound **1** and ∼25.4 kJ/mol for compound **2**. These two values are of medium grade, in comparison with those reported previously (8−54 kJ/mol).[5] Aforementioned calculational results imply that the compounds that we designed may be synthesized by experiment, and consequent experimental results prove this conclusion to be correct. Generally, the BSSE has an important role in the DFT computations, particularly for hydrogen-bonded complexes.[42] Here, the proportions of BSSE to the corrected interaction energies $E_{C,ZPEc}$ are 32.11% for **1** and 32.38% for **2**, which indicates that the BSSE corrections for the interaction energies are necessary.

Comparison of the values in parentheses in Table 4, which were calculated at the B3LYP/6-31G** level, with those calculated at the B3LYP/6-31G* level, gives differences of 4.0 kJ for compound **1** and 4.7 kJ for compound **2**. The errors are all <5%, which did not influence our conclusions and indicated that calculational precision with the 6-31G* basis set was satisfactory for the system we studied here.

TABLE 5: Selected Molecular Structure Parameters

Compound **1**				Compound **2**			
	experimental	calculated	error[a]		experimental	calculated	error[a]
			Bond Lengths (Å)				
O(1)−C(7)	1.329(3)	1.331	0.002	O(1)−C(9)	1.313(4)	1.334	0.021
O(2)−C(7)	1.221(3)	1.232	0.011	O(2)−C(9)	1.218(3)	1.234	0.016
O(3)−N(1)	1.398(2)	1.375	−0.023	O(3)−N(1)	1.382(3)	1.374	−0.008
N(1)−C(8)	1.291(3)	1.293	0.002	N(1)−C(11)	1.280(4)	1.293	0.013
C(1)−C(6)	1.391(3)	1.402	0.011	C(1)−C(6)	1.381(4)	1.408	0.027
C(1)−C(2)	1.399(4)	1.393	−0.006	C(1)−C(2)	1.382(4)	1.407	0.025
C(2)−C(3)	1.380(4)	1.397	0.017	C(1)−C(7)	1.463(4)	1.464	0.001
C(3)−C(4)	1.382(4)	1.398	0.016	C(2)−C(3)	1.388(4)	1.393	0.005
C(4)−C(5)	1.379(3)	1.392	0.013	C(3)−C(4)	1.363(4)	1.395	0.032
C(5)−C(6)	1.393(3)	1.402	0.009	C(4)−C(5)	1.364(5)	1.399	0.035
C(6)−C(7)	1.482(3)	1.486	0.004	C(5)−C(6)	1.388(4)	1.390	0.002
C(9)−C(8)	1.502(3)	1.505	0.003	C(7)−C(8)	1.317(4)	1.347	0.030
C(8)−C(8A)	1.476(4)	1.477	0.001	C(8)−C(9)	1.456(4)	1.470	0.014
				C(10)−C(11)	1.499(4)	1.505	0.006
				C(11)−C(11A)	1.472(6)	1.477	0.005
			Bond Angles (deg)				
C(8)−N(1)−O(3)	112.7(8)	115.0	2.3	C(11)−N(1)−O(3)	112.3(3)	115.1	2.8
C(6)−C(1)−C(2)	120.0(2)	119.8	−0.2	C(6)−C(1)−C(2)	117.4(3)	118.3	0.9
C(3)−C(2)−C(1)	119.5(2)	120.1	−0.6	C(6)−C(1)−C(7)	122.2(3)	123.1	0.9
C(2)−C(3)−C(4)	120.3(2)	120.2	−0.1	C(2)−C(1)−C(7)	120.3(3)	118.6	−1.7
C(5)−C(4)−C(3)	120.8(2)	120.0	−0.8	C(1)−C(2)−C(3)	121.4(3)	121.0	−0.4
C(4)−C(5)−C(6)	119.6(2)	120.0	0.4	C(4)−C(3)−C(2)	120.6(3)	119.9	−0.7
C(1)−C(6)−C(5)	119.9(2)	119.9	0.0	C(3)−C(4)−C(5)	118.8(3)	119.7	0.9
C(1)−C(6)−C(7)	122.1(2)	121.6	−0.5	C(4)−C(5)−C(6)	121.2(3)	120.3	−0.9
C(5)−C(6)−C(7)	118.0(2)	118.5	0.5	C(1)−C(6)−C(5)	120.7(3)	120.7	0.0
O(2)−C(7)−O(1)	122.4(2)	123.2	0.8	C(8)−C(7)−C(1)	128.4(3)	127.2	−1.2
O(2)−C(7)−C(6)	123.8(2)	122.5	−1.3	C(7)−C(8)−C(9)	125.2(3)	123.4	−1.8
O(1)−C(7)−C(6)	113.8(2)	114.3	0.5	O(2)−C(9)−O(1)	120.9(3)	123.3	2.4
N(1)−C(8)−C(8A)	114.2(2)	115.6	1.4	O(2)−C(9)−C(8)	124.0(3)	121.4	−2.6
N(1)−C(8)−C(9)	124.2(2)	123.6	−0.6	O(1)−C(9)−C(8)	115.1(3)	115.3	0.2
C(8A)−C(8)−C(9)	121.6(2)	120.7	−0.9	N(1)−C(11)−C(11A)	113.8(3)	115.6	1.8
				N(1)−C(11)−C(10)	125.3(3)	123.6	−1.7
				C(11A)−C(11)−C(10)	120.9(3)	120.7	−0.2
			Torsion Angles (deg)				
C(1)−C(6)−C(7)−O(1)	10.22	0.00	−10.22	C(2)−C(1)−C(7)−C(8)	179.67	171.08	−8.59
C(1)−C(6)−C(7)−O(2)	−169.45	−179.99	−10.54	C(6)−C(1)−C(7)−C(8)	0.46	9.40	8.94
C(5)−C(6)−C(7)−O(1)	−170.73	−179.99	−9.26	C(1)−C(7)−C(8)−C(9)	−179.20	−179.18	0.02
C(5)−C(6)−C(7)−O(2)	9.60	0.01	−9.59	C(7)−C(8)−C(9)−O(1)	2.21	2.32	0.11
				C(7)−C(8)−C(9)−O(2)	−177.99	−177.93	0.06
				C(10)−C(11)−N(1)−O(3)	−1.33	−0.13	1.20
				C(11A)−C(11)−N(1)−O(3)	179.08	179.79	0.71

[a] Error = calculated value − experimental value. Symmetry transformations used to generate equivalent atoms are as follows: A is $-x+1, -y+1, -z$ for **1**, and A is $-x+2, -y+1, -z$ for **2**, respectively.

TABLE 6: Hydrogen Bond Distances and Angles for 1 and 2

	D−H (Å)		H−A (Å)		D···A (Å)		∠D−H···A (deg)	
D−H···A	experimental	calculated	experimental	calculated	experimental	calculated	experimental	calculated
				Compound **1**				
O(3)−H(3)···O(2)	0.820	0.993	1.956	1.742	2.729	2.719	157.1	167.0
O(1)−H(1)···N(1)	0.993	1.006	1.803	1.781	2.781	2.779	171.4	171.1
				Compound **2**				
O(3)−H(3)···O(2)	0.820	0.994	1.953	1.734	2.724	2.713	156.3	167.3
O(1)−H(1)···N(1)	0.997	1.005	1.766	1.782	2.752	2.779	168.7	170.6

3.2. Crystal Structures and Optimized Geometries. The proposed structure and the experimental structure of compounds **1** and **2**, with the atomic numbering, are shown in Figures 1 and 2, respectively. Figures 3 and 4 each respectively show a perspective view of the crystal packing in the unit cell of compounds **1** and **2**. Some selected single-crystal X-ray diffraction data, together with the optimized geometrical parameters at the B3LYP/6-31G* level, are listed in Table 5. The experimental and calculated hydrogen-bond distances and angles are listed in Table 6. More structural information about compounds **1** and **2** is given in the Supporting Information.

The crystal structures of the compounds closely resemble the proposed structures, which are evidence that we have successfully applied theoretical models to real-world synthesis of the supramolecular compounds.

According to the data of crystal structures, the crystal lattices of supramolecular compounds **1** and **2** are similar, which all comprise two trimer molecules in the unit cell. Each symmetric trimer molecule consists of two BZA or CINA molecules and one DIMG molecule, and the three monomers are connected by quadruple intermolecular hydrogen bonds. All the bond lengths and angles of DIMG and BZA or CINA are in the

TABLE 7: Mulliken Atomic Charges of the Monomers and the Compounds 1 and 2 at the B3LYP/6-31G* Level

atom	BZA	DMG	compound **1**	atom	CINA	DMG	compound **2**
	Atomic Charge (e)				Atomic Charge (e)		
C(1)	−0.1595		−0.1566	C(1)	0.1683		0.1654
C(2)	−0.1356		−0.1360	C(2)	−0.1870		−0.1854
C(3)	−0.1170		−0.1164	C(3)	−0.1309		−0.1311
C(4)	−0.1372		−0.1369	C(4)	−0.1234		−0.1230
C(5)	−0.1542		−0.1530	C(5)	−0.1310		−0.1312
C(6)	0.0696		0.0686	C(6)	−0.1715		−0.1708
C(7)	0.5360		0.5596	C(7)	−0.1528		−0.1500
O(1)	−0.5832		−0.6228	C(8)	−0.1983		−0.1966
O(2)	−0.4744		−0.5303	C(9)	0.5772		0.5986
H(1B)	0.4117		0.4707	O(1)	−0.5878		−0.6278
H(1A)	0.1613		0.1624	O(2)	−0.4847		−0.5383
H(2A)	0.1384		0.1394	H(1A)	0.4085		0.4688
H(3A)	0.1389		0.1396	H(2)	0.1382		0.1393
H(4A)	0.1397		0.1402	H(3B)	0.1380		0.1388
H(5A)	0.1655		0.1649	H(4)	0.1380		0.1385
				H(5)	0.1386		0.1389
				H(6)	0.1395		0.1398
				H(7)	0.1671		0.1691
				H(8)	0.1541		0.1541
N(1)		−0.2517	−0.2937	N(1)		−0.2517	−0.2932
O(3)		−0.4998	−0.5213	O(3)		−0.4998	−0.5223
H(3B)		0.4192	0.4569	H(3A)		0.4192	0.4559
C(8)		0.3100	0.3398	C(11)		0.3100	0.3388
C(9)		−0.5151	−0.5390	C(10)		−0.5151	−0.5383
H(9A)		0.1875	0.2042	H(10D)		0.1875	0.2029
H(9B)		0.1749	0.1799	H(10E)		0.1749	0.1783
H(9C)		0.1749	0.1798	H(10F)		0.1749	0.1796

TABLE 8: Intermolecular Natural Bond Orbitals Interacting and the Corresponding Stable Energy[a]

donor	acceptor	energy, *E* (kJ/mol)
	Compound **1**	
LP(1) O(2)	BD* O(3)−H(3B)	35.2
LP(2) O(2)	BD* O(3)−H(3B)	77.9
LP(1) N(1)	BD* O(1)−H(1B)	134. 3
	Compound **2**	
LP(1) O(2)	BD* O(3)−H(3A)	34.8
LP(2) O(2)	BD* O(3)−H(3A)	84.1
LP(1) N(1)	BD* O(1)−H(1A)	132.9

[a] LP means lone pair; BD* represents antibond.

normal range and are all in agreement with those of related structures reported earlier.[43−45] For BZA in **1**, the C(7) atoms with a phenyl ring define a plane where the largest atomic deviation is 0.008 Å. The C(6) atoms with a carboxylic group are also quite planar, and the largest atomic deviation from the least-squares plane is 0.002 Å. The dihedral angle between the aforementioned two planes is 9.93°. In compound **2**, no atoms are coplanar. The quadruple hydrogen bonds are divided into two types: one is formed between the acceptor O(2) atoms of BZA or CINA with O(3) atoms in DIMG, and the other is formed between the acceptor N(1) atoms of DIMG with O(1) atoms in BZA or CINA.

To compare the optimized geometric parameters with the experimental data in Table 5, we find that most of the optimized bond lengths are slightly larger than the experimental values, which are due to the fact that the theoretical calculations belong to isolated molecules in the gaseous phase at 0 K and the experimental results belong to molecules in the solid phase.The largest deviations of bond lengths and angles between the theoretical and experimental geometry are 0.023 Å and 2.3° for **1**, and 0.035 Å and 2.8° for **2**, respectively, which indicate that the calculational precision is satisfactory.[46] On the other hand, the changes of the torsion angles are bigger than those of bond angles. In compound **1**, the largest change of the torsion angle is 10.54°, and the changes occur mainly on the atoms

TABLE 9: Selected Vibrational Frequencies

Frequency (cm^{-1})		
experimental	calculated	description[a]
	Compound **1**	
3250−3100	3202	DIMG −OH (str)
3072	3105−3072	BZA ip phenyl ring C−H (def)
3000	2954−2947	BZA −OH (str)
1689	1689	BZA C═O (str) + all −OH (def)
1636	1642	DIMG N═C (str).+ all −OH (def)
1603	1597−1575	BZA phenyl ring skeleton (def)
1500	1521−1500	DIMG −OH (def)
1425	1419−1440	BZA ip phenyl ring C−H (def)
1305	1303−1304	BZA ip phenyl ring C−H (def)
1276	1290	BZA C(6)−C(7) (str)
1018	1019	DIMG N−O (str)
930	905	BZA −OH (def)
770	753	DIMG −OH (def)
	Compound **2**	
3209	3179	all −OH (str)
3000	3044−3000	all C−H (str)
2901	2971	all −OH (str)
1682	1688	CINA C═O (str) + all −OH (def)
1623	1643−1647	DIMG C═N (str.) + all −OH (def)
1600	1623	CINA C═C (str)
1577	1594−1569	phenyl ring skeleton (def)
1499	1512	DIMG skeleton (def) + all −OH (def)
1451	1463−1460	DIMG $-CH_3$ (def) + all −OH (def)
1325	1331	CINA C═C (str)
1286	1296−1245	CINA $-CH_3$ (def) + −OH (def)
1158	1167	C−H (def) on phenyl ring +C═C
1140	1147	oop phenyl ring C−H (def)
1032	1018	DIMG C═N (str)
997	1016	ip phenyl ring C−H (def)
925	925	CINA C(8)−C(9) (str)
897	892	all −OH (def)
775	762	DIMG −OH (def)
686	690	C−H (def) on phenyl ring +C═C
592	578	CINA skeleton (def)

[a] Atomic numbering as shown in Figures 1 and 2. Legend of bond types is as follows: str, stretch; ip, in-plane; oop, out-of-plane; def, deformation.

TABLE 10: Thermodynamic Properties of the Monomers and Compounds at Different Temperatures[a]

temperature, T (K)	heat capacity, $C^0_{p,m}$ (J mol^{-1} K^{-1})	entropy, S^0_m (J mol^{-1} K^{-1})	enthalpy, H^0_m (kJ/mol	change in entropy, ΔS_T (J mol^{-1} K^{-1})[a]	change in enthalpy, ΔH_T (kJ/mol)[b]	change in Gibbs free energy, ΔG_T (kJ/mol)[c]
			BZA			
200.00	87.6	314.0	11.2			
298.15	126.8	356.2	21.7			
400.00	164.7	398.9	36.6			
500.00	195.3	439.1	54.7			
600.00	219.6	476.9	75.5			
700.00	238.9	512.3	98.4			
800.00	254.5	545.2	123.1			
			DIMG			
200.00	115.1	344.7	14.7			
298.15	149.6	397.2	27.7			
400.00	182.2	445.8	44.6			
500.00	209.5	489.5	64.2			
600.00	232.2	529.7	86.4			
700.00	251.0	567.0	110.6			
800.00	266.8	601.6	136.5			
			Compound **1**			
200.00	303.6	666.0	37.6	−306.7	−132.8	−71.5
298.15	417.7	808.4	73.0	−301.2	−131.5	−41.7
400.00	528.6	947.0	121.3	−296.6	−129.9	−11.3
500.00	620.1	1075.2	178.9	−292.5	−128.1	18.2
600.00	694.0	1195.0	244.8	−288.5	−125.9	47.2
700.00	754.0	1306.6	317.3	−285.0	−123.5	76.0
800.00	803.2	1410.6	395.2	−281.4	−120.9	104.2
			CINA			
200.00	113.9	360.4	14.6			
298.15	162.4	414.8	28.1			
400.00	209.8	469.4	47.1			
500.00	248.4	520.5	70.1			
600.00	279.2	568.6	96.6			
700.00	303.8	613.6	125.7			
800.00	323.9	655.5	157.2			
			Compound **2**			
200.00	355.3	759.0	44.1	−306.5	−133.8	−72.5
298.15	488.1	925.5	85.4	−301.3	−132.5	−42.7
400.00	618.3	1087.6	141.9	−297.0	−131.0	−12.2
500.00	725.9	1237.5	209.3	−293.0	−129.2	17.3
600.00	813.0	1377.8	286.4	−289.1	−127.1	46.4
700.00	883.6	1508.6	371.4	−285.6	−124.7	75.2
800.00	941.7	1630.5	462.7	−282.1	−122.1	103.4

[a] $\Delta S_T = (S^0_m)_{\text{trimer}} - 2(S^0_m)_{\text{BZA or CINA}} - (S^0_m)_{\text{DIMG}}$. [b] $\Delta H_T = (H^0_m + E + \text{ZPE})_{\text{trimer}} - 2(H^0_m + E + \text{ZPE})_{\text{BZA or CINA}} - (H^0_m + E + \text{ZPE})_{\text{DIMG}}$. [c] $\Delta G_T = \Delta H_T - T\Delta S_T$ and the scale factor for frequencies is 0.96.

involved in hydrogen bonds in BZA. In compound **2**, the biggest change in torsion angle is 8.94°, which occurs in CINA on double-bond sites rather than on the carboxylic groups, because twisting the C(7)−C(8) double bond is much easier than twisting the carboxylic groups. These phenomena can be explained as follows: in a gaseous-phase state, each molecule exists as an isolated one; thus, to form hydrogen bonds between the BZA or CINA and the DIMG, it is sufficient to change only the bond lengths and bond angles of DIMG. However, in the crystal state, the close packing of all the molecules and the existence of the crystal fields forces the BZA or CINA to have some twists, except for the structure changes of DIMG, to adapt to the highly selective and directional nature of quadruple hydrogen bonds. The energy cost of changing the structure of the BZA or the CINA and the DIMG certainly must be smaller than the energies offered by quadruple hydrogen bonds used to stabilize the compounds.

In addition, as observed from the hydrogen bond distances and angles in Table 6, the distances between the donors and acceptors in the crystal structures are very similar to those in the proposed structures, and the biggest deviation is only 0.027 Å, which also proves that our original design idea is correct.

In summary, by comparing the optimized values with experimental results, we can draw a conclusion that the B3LYP/6-31G* level is suitable for the system studied here. Thus, the discussion above and thereafter is derived from the optimized structures using this level.

3.3. Atomic Charges and Charge Transfer. The Mulliken atomic charges of the monomers and compounds **1** and **2**, which have been calculated at the B3LYP/6-31G* level, are listed in Table 7. (Only half of the atoms are listed in view of the symmetry.)

The charge redistribution mainly occurs among the atoms involved in hydrogen bonds. The charges of all the donors and acceptors increase, and, accordingly, the charges of atoms in contact with the donors and acceptors decrease. On the other hand, in the BZA and CINA, the changes in the atomic charge in a phenyl ring are not evident, which mainly occur in the carboxyl group adjacent to the DIMG. However, all the atoms in the DIMG have changes in atomic charge, to some extent. These phenomena show the cooperation effects in the interaction of the trimers. In a word, after forming quadruple hydrogen bonds, the net results of charge transfer are that, for compound **1**, the BZA acquires 0.0066 e and the DIMG loses 0.0132 e;

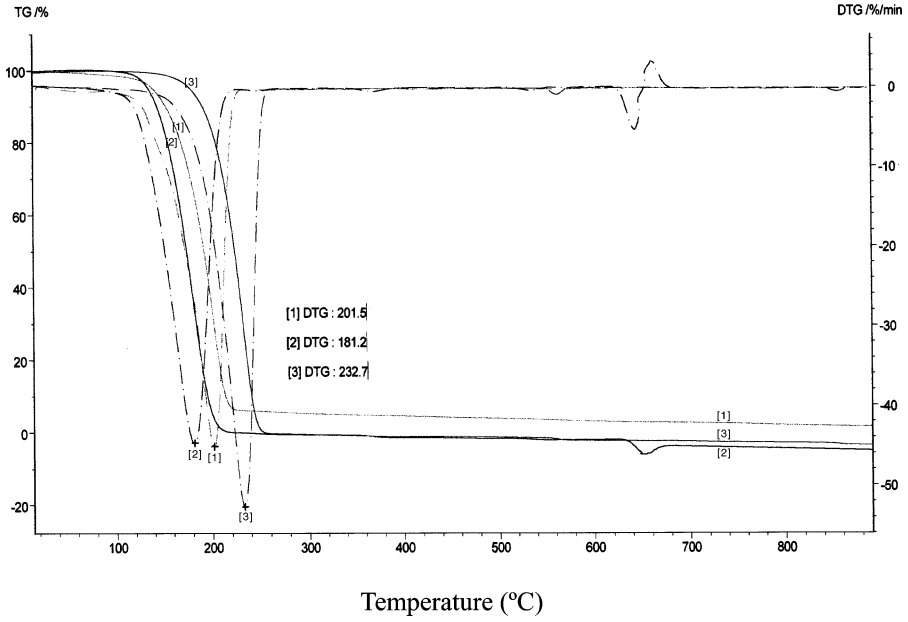

Figure 5. Thermogravimetry/differential thermogravimetry (TG/DTG) curves of compound **1** (curve [1]), BZA (curve [2]), and DIMG (curve [3]).

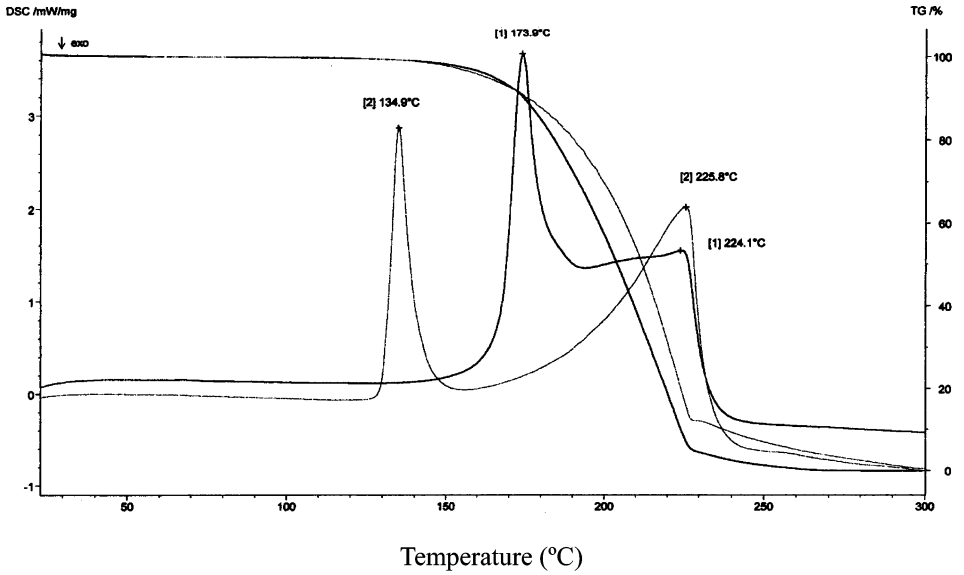

Figure 6. TG/DSC curves of compound **2** (curve [1]) and CINA (curve [2]).

for compound **2**, the CINA acquires 0.0017 e and the DIMG loses 0.0034 e. The dipole moment of compound **1** is 0 D. For compound **2**, the dipole moment is 0.0592 D, which may be caused by the minor twisting of compound **2** in the calculations.

3.4. Natural Bond Orbital Analysis. To probe the origin of the interaction, natural bond orbital (NBO) analyses at the B3LYP/6-31G* level were performed. The donor and acceptor (here, donor = donor electrons and acceptor = accept electrons) of NBOs between intermolecules, and their interacting stable energies, are collected in Table 8. The stable energies are proportional to the NBO interacting intensities. For these two compounds, the O(2) atom of the BZA or CINA donates its first and second lone-pair electrons to the O(3)−H(3B) or O(3)−H(3A) antibonds of DIMG and gives stable energies. The N(1) atom of DIMG donates one lone-pair electron to O(1)−H(1B) antibonds of the BZA or to O(1)−H(1A) antibonds of the CINA and gives stable energies. In compounds **1** and **2**, the strengths of O−H···N are much larger than those of O−H···O. According to Table 6, the distances of O−H···N are longer than the distances of O−H···O, but the angles of O−H···N are nearer to 180° than those of O−H···O, which are more suitable for overlap orientation for the hydrogen bond and create the differences of interacting intensities between the two types of hydrogen bonds.

3.5. IR Spectra. Some calculated harmonic frequencies are shown in Table 9 and compared with the experimental data. The calculated vibrational frequencies were scaled by 0.96.[41] Descriptions concerning the assignment have also been indicated in this table. The Gauss-view program[47] was used to assign the calculated harmonic frequencies.

Comparison of the differences between the predictions for compounds **1** or **2** and the experimental frequencies reveals good agreement, with the predicted frequencies differing by ∼1.5% from the experimental frequencies, most of the former being slightly larger. The most significant feature is the modes of −OH stretch vibration in compounds **1** and **2**, which exhibit a large red shift, with respect to those in their respective monomers. These phenomena are caused by the formation of quadruple hydrogen bonds in the supramolecules.

3.6. Thermodynamic Properties. On the basis of vibrational analysis and statistical thermodynamics, the standard thermodynamic functions—heat capacity ($C^0_{p,m}$), entropy (S^0_m), and enthalpy (H^0_m)—were obtained and are listed in Table 10. For each of the compounds, the magnitudes of the $C^0_{p,m}$ values are slightly larger than the sums of the $C^0_{p,m}$ values of three monomers at each temperature. In the course of the transformation of the monomers to the compound, both the entropy and enthalpy decrease at any temperature from 200.00 K to 800.00 K ($\Delta S_T < 0$, $\Delta H_T < 0$) and their changes decrease as T increases. Therefore, the intermolecular interactions are exothermic processes that are accompanied by a decrease in the degree of confusion. From the equation

$$\Delta G_T = \Delta H_T - T\Delta S_T$$

the Gibbs free energy change (ΔG_T) in the processes are from negative to positive. From $T = 200.00$ K to $T = 400.00$ K, $\Delta G_T < 0$, which implies that compounds **1** and **2** form via spontaneous processes. At 298.15 K on the calculation model of an ideal gas, the calculated equilibrium constants, based on the equation

$$\Delta G_T = -RT \ln K_p$$

are 2.02×10^7 for **1** and 3.33×10^7 for **2**. This observation indicates that the trimers are the main component at this temperature. From 500.00 K to 800.00 K and thereafter, $\Delta G_T > 0$, which demonstrates that the processes of formation for compounds **1** and **2** are not spontaneous. According to the data and the changes of ΔS_T, ΔH_T, and ΔG_T, it can be seen that, in the temperature range from 200.00 K to 400.00 K, the values of ΔH_T mainly determine the values of ΔG_T and determine whether the trimer formation reactions are spontaneous or not. After 500.00 K, the magnitudes of ΔG_T are mainly determined by $T\Delta S_T$. Based on the values of ΔS_T and ΔH_T, the transition temperatures of these two spontaneous reactions are 438.0 K for compound **1** and 441.1 K for compound **2**. Although the aforementioned conclusions are drawn based on the gaseous-phase state structures, they provide useful references for our designs of the synthesis of the heterotrimer supramolecules under experimental conditions. Our research groups obtained the anticipatory compounds successfully and made the proposed thermodynamic spontaneous reactions become true by controlling the synthetic conditions and selecting catalysts and constructed two new supramolecular materials creatively.

According to the data in Table 10 for compounds **1** and **2**, the correlations between the thermodynamic properties $C^0_{p,m}$ and S^0_m and temperature T are described. Based on these relationships, one can obtain the values of $C^0_{p,m}$ and S^0_m at any other temperatures. For **1**,

$$C^0_{p,m} = 18.8487 + 1.5647T - (7.3166 \times 10^{-4})T^2$$

$$S^0_m = 438.4429 + 1.2406T$$

and for **2**,

$$C^0_{p,m} = 22.3377 + 11.8268T - (8.4814 \times 10^{-4})T^2$$

$$S^0_m = 492.4482 + 1.4520T$$

3.7. Thermogravimetric Analysis and Differential Scanning Calorimetry. The curves of the thermogravimetric (TG) analysis and differential thermal gravimetric (DTG) analysis for compound **1** and the curves of the TG analysis and differential scanning calorimetry (DSC) analysis for compound **2** are shown in Figures 5 and 6, respectively. It can be seen that the thermal properties of compounds **1** and **2** are different from their original compounds DIMG, BZA, and CINA. They have different decomposition temperatures. As observed from Figure 5, in the solid state, the existence of the crystal field, along with the quadruple hydrogen bonds, have connected the three monomers together so closely that compound **1** has become a new complex and has only one decomposition temperature. On the other hand, to compare the experimental decomposition temperature of compound **1** (201.5 °C) with the calculated spontaneous reaction transition temperature (164.8 °C), it is also clear that the existence of the crystal field has increased the stability of compound **1**. In Figure 6, similar phenomena can be found for compound **2**, where the experimental decomposition temperature is 173.9 °C, and the calculated spontaneous reaction transition temperature is 168.1 °C. To compare compounds **1** and **2** with their original compounds, we can conclude that **1** and **2** are not the ordinary superposition of the monomers and they have become new complexes different from the original monomers.

4. Conclusions

Under the guidance of the calculational results, we have successfully synthesized two new supramolecular compounds: dimethylglyoxime·benzoic acid (DIMG·2BZA) and dimethylglyoxime·cinnamic acid (DIMG·2CINA). Also, we have determined that $FeCl_3$ is the best catalyst. The crystal structures of the compounds closely resemble the proposed structures. IR spectra analyses show that the predicted vibrational frequencies are in good agreement with the experimental values. Thermal stability analyses demonstrate that these two supramolecular compounds are new complexes, and they are not the ordinary superposition of the original monomers. We hope our research will be helpful to the further study of supramolecular complexes. In addition, we hope our investigations can provide new information for constructing novel multicomponent self-assembly supramolecular materials.

Supporting Information Available: Two CIF files **S1** and **S2** containing structural data of compounds **1** and **2** (CIF). This material is available free of charge via the Internet at http://pubs.acs.org.

References and Notes

(1) Lehn, J. M. *Angew. Chem., Int. Ed. Engl.* **1988**, *27*, 89.
(2) Lehn, J. M. *Angew. Chem., Int. Ed. Engl.* **1990**, *29*, 1304.
(3) Chen, C. T.; Sustick, K. S. *Coord. Chem. Rev.* **1993**, *128*, 293.
(4) Arends, I. W. C. E.; Sheldon, R. A.; Wallau, M.; Schuchardt, U. *Angew. Chem., Int. Ed. Engl.* **1997**, *36*, 1145.
(5) Philp, D.; Stoddart, J. F. *Angew. Chem., Int. Ed. Engl.* **1996**, *35*, 1155.
(6) Colquhoun, H. M.; Stoddart, J. F.; Williams, D. J. *Angew. Chem.* **1986**, *98*, 483 (in Ger.); *Angew. Chem., Int. Ed. Engl.* **1986**, *25*, 487.
(7) Gallant, M.; Viet, M. T. P.; Wuest, J. D. *J. Am. Chem. Soc.* **1991**, *113*, 721. Gallant, M.; Viet, M. T. P.; Wuest, J. D. *J. Org. Chem.* **1991**, *56*, 2284.
(8) Simard, M.; Su, J. D.; Wuest, J. D. *J. Am. Chem. Soc.* **1991**, *113*, 4696. Hajek, F.; Graf, E.; Hosseini, M. W.; Delaigue, X.; De Cian, A.; Fischer, J. *Tetrahedron Lett.* **1996**, *37*, 1401. Hosseini, M. W.; Brand, G.; Schaeffer, P.; Ruppert, R.; De Cian, A.; Fischer, J. *Tetrahedron Lett.* **1996**, *37*, 1405.
(9) Sherrington, D. C.; Taskinen, K. A. *Chem. Soc. Rev.* **2001**, *30*, 83.
(10) Lawrence, D. S.; Jiang, T.; Levitt, M. *Chem. Rev.* **1995**, *95*, 2229.
(11) Beijer, F. H.; Sijbesma, R. P.; Koojman, H.; Spek, A. L.; Meijer, E. W. *J. Am. Chem. Soc.* **1998**, *120*, 6761.
(12) Januky, W.; Hosseini, M. W.; Plaeix, J. M.; de Cian, A.; Kyritsakas, N.; Fischer, J. *Chem. Commun.* **1999**, 2313.

(13) Zhang, Y.; Guo, Z. J.; You, X. Z. *J. Am. Chem. Soc*. **2001**, *123*, 9378.
(14) Labanowski, J. K.; Andzelm, J. *Density Functional Methods in Chemistry*; Springer−Verlag: New York, 1991.
(15) Fitzgerald, G.; Andzelm, J. *J. Phys. Chem.* **1991**, *95*, 10531.
(16) Ziegler, T. *Pure Appl. Chem*. **1991**, *63*, 873.
(17) Andzelm, J.; Wimmer, E. *J. Chem. Phys*. **1992**, *95*, 1208.
(18) Scuseria, G. E. *J. Chem. Phys.* **1992**, *97*, 7528.
(19) Dickson, R. M.; Becke, A. D. *J. Chem. Phys.* **1993**, *99*, 3898.
(20) Johnson, B. G.; Gill, P. M. W.; Pople, J. A. *J. Chem. Phys.* **1993**, *98*, 5612.
(21) Oliphant, N.; Bartlett, R. J. *J. Chem. Phys.* **1994**, *100*, 6550.
(22) Sim, F.; St-Amant, F. A.; Papai, I.; Salahub, D. R. *J. Am. Chem. Soc*. **1992**, *14*, 4391.
(23) Zhang, Q.; Bell, R.; Truong, T. N. *J. Phys. Chem.* **1995**, *99*, 592.
(24) Frisch, M. J.; Trucks, G. W.; Schlegel, H. B.; Scuseria, G. E.; Robb, M. A.; Cheeseman, J. R.; Zakrzewski, V. G.; Montgomery, J. A., Jr.; Stratmann, R. E.; Burant, J. C.; Dapprich, S.; Millam, J. M.; Daniels, A. D.; Kudin, K. N.; Strain, M. C.; Farkas, O.; Tomasi, J.; Barone, V.; Cossi, M.; Cammi, R.; Mennucci, B.; Pomelli, C.; Adamo, C.; Clifford, S.; Ochterski, J.; Petersson, G. A.; Ayala, P. Y.; Cui, Q.; Morokuma, K.; Malick, D. K.; Rabuck, A. D.; Raghavachari, K.; Foresman, J. B.; Cioslowski, J.; Ortiz, J. V.; Stefanov, B. B.; Liu, G.; Liashenko, A.; Piskorz, P.; Komaromi, I.; Gomperts, R.; Martin, R. L.; Fox, D. J.; Keith, T.; Al-Laham, M. A.; Peng, C. Y.; Nanayakkara, A.; Gonzalez, C.; Challacombe, M.; Gill, P. M. W.; Johnson, B. G.; Chen, W.; Wong, M. W.; Andres, J. L.; Head-Gordon, M.; Replogle, E. S.; Pople, J. A. *Gaussian 98*, revision A.7; Gaussian, Inc.: Pittsburgh, PA, 1998.
(25) Becke, A. D. *J. Chem. Phys*. **1993**, *98*, 5648.
(26) Lee, C.; Yang, W.; Parr, R. G. *Phys. Rev. B* **1988**, *B37*, 785.
(27) Sosa, C.; Andzelm, J.; Elkin, B. C.; Winner, E.; Dobbs, K. D.; Dixon, D. A. *J. Phys. Chem*. **1992**, *96*, 6630.
(28) Murray, C. W.; Laming, G. J.; Handy, N. C.; Amos, R. D. *J. Phys. Chem*. **1993**, *97*, 1868.
(29) Hutter, J.; Luthi, H. P.; Diederich, F. *J. Am. Chem. Soc*. **1994**, *116*, 750.
(30) Binkley, J. S.; Pople, J. A.; Hehre, W. J. *J. Am. Chem. Soc*. **1980**, *102* (2), 939.
(31) Gordon, M. S.; Binkley, J. S.; Pople, J. A.; Pietro, W. J.; Hehre, W. J. *J. Am. Chem. Soc*. **1982**, *104*, 2797.
(32) Peng, C.; Ayala, P. Y.; Schlegel, H. B.; Frisch, M. J. *J. Comput. Chem*. **1996**, *17*, 49.
(33) Boys, S. F.; Bernardi, F. *Mol. Phys*. **1970**, *19*, 553.
(34) Johansson, A.; Kollman, P.; Rothenberg, S. *Theor. Chim. Acta* **1973**, *29*, 167.
(35) Chalasinski, G.; Szczesniak, M. M. *Mol. Phys.* **1988**, *63*, 205.
(36) Muguet, F. F.; Robinson, G. W. *J. Chem. Phys*. **1995**, *102*, 3648.
(37) Reed, A. E.; Weinstock, R. B.; Weinhold, F. *J. Chem. Phys*. **1985**, *83*, 735.
(38) Sheldrick, G. M. *SAINT v4 Software Reference Manual*; Siemens Analytical X-ray Systems, Inc.: Madison, WI, 1996.
(39) Sheldrick, G. M., *SHELXTL, v5 Reference Manual*; Siemens Analytical X-ray Systems, Inc.: Madison, WI, 1996.
(40) Wilson, A. J. *International Table for X-ray Crystallography*; Kluwer Academic Publishers: Dordrecht, The Netherlands, 1992; Vol. C, Tables 6.1.1.4 (pp 500−502) and 4.2.6.8 (pp 219−222).
(41) Pople, J. A.; Schlegel, H. B.; Krishnan, R.; Defrees, D. J.; Binkley, J. S.; Frisch, M. J.; Whiteside, R. A.; Hout, R. F.; Hehre, W. J. *Int. J. Quantum Chem., Quantum Chem. Symp.* **1981**, *15*, 269.
(42) Novoa, J. J.; Sosa, C. *J. Phys. Chem*. **1995**, *99*, 15837.
(43) Jian, F. F.; Sun, P. P.; Xiao, H. L. *Chin. J. Inorg. Chem.* **2003**, *19* (7), 757.
(44) Zhao, P. S.; Jian, F. F.; Lu, L. D.; Yang, X. J.; Wang, X.; Raj, S. S.; Fun, H. K. *Chin. J. Inorg. Chem.* **2000**, *16* (6), 964.
(45) Wang, Z. X.; Jian, F. F.; Zhang, Y. R.; Li, F. S.; Fun, H. K.; Chinnakali, K. *J. Chem. Crystallogr*. **1999**, *29* (8), 885.
(46) Xiao, J. J.; Zhang, J.; Yang, D.; Xiao, H. M. *Huaxue Xuebao* **2002**, *60*, 2110.
(47) Frish, A.; Nielsen, A. B.; Holder, A. J. *Gauss-view Users Manual*; Gaussian, Inc.: Pittsburgh, PA, 2000.